Electrochemistry

Deutsche Ausgabe: DOI: 10.1002/ange.201604160
Internationale Ausgabe: DOI: 10.1002/anie.201604160

An Aurivillius Oxide Based Cathode with Excellent CO_2 Tolerance for Intermediate-Temperature Solid Oxide Fuel Cells

Yinlong Zhu, Wei Zhou, Yubo Chen, and Zongping Shao**

Abstract: *The Aurivillius oxide $Bi_2Sr_2Nb_2MnO_{12-\delta}$ (BSNM) was used as a cobalt-free cathode for intermediate-temperature solid oxide fuel cells (IT-SOFCs). To the best of our knowledge, the BSNM oxide is the only alkaline-earth-containing cathode material with complete CO_2 tolerance that has been reported thus far. BSNM not only shows favorable activity in the oxygen reduction reaction (ORR) at intermediate temperatures but also exhibits a low thermal expansion coefficient, excellent structural stability, and good chemical compatibility with the electrolyte. These features highlight the potential of the new BSNM material as a highly promising cathode material for IT-SOFCs.*

The importance of transforming our highly fossil-fuel-dependent society into one that depends on green, renewable energy to achieving sustainable development has been recognized, and electrochemical energy conversion and storage will play crucial roles in this transformation.[1] During the past decades, solid oxide fuel cells (SOFCs), as high-temperature electrochemical energy-conversion devices, have attracted particular attention owing to their high energy-conversion efficiency, excellent fuel flexibility, and environmental friendliness.[2] However, the widespread application of SOFC technology requires it to be competitive in terms of associated costs with current mature power-generation technologies based on combustion and to have a long lifetime. The reduction of the operating temperature from conventional 1000 °C to the intermediate range of 600–800 °C may greatly accelerate the commercialization of SOFC technology by reducing the system costs, increasing the operational lifetime, and shortening the start-up time.[3]

[*] Y. L. Zhu, Prof. W. Zhou, Dr. Y. B. Chen
Jiangsu National Synergetic Innovation Center for Advanced Materials (SICAM)
State Key Laboratory of Materials-Oriented Chemical Engineering
College of Chemical Engineering
Nanjing Tech University
No. 5 Xin Mofan Road, Nanjing 210009 (P.R. China)
E-mail: zhouwei1982@njtech.edu.cn
Prof. Z. P. Shao
Jiangsu National Synergetic Innovation Center for Advanced Materials (SICAM)
State Key Laboratory of Materials-Oriented Chemical Engineering
College of Energy, Nanjing Tech University
No. 5 Xin Mofan Road, Nanjing 210009 (P.R. China)
and
Department of Chemical Engineering, Curtin University
Perth, Western Australia 6845 (Australia)
E-mail: shaozp@njtech.edu.cn

Supporting information for this article can be found under: http://dx.doi.org/10.1002/anie.201604160.

As the activation of oxygen is much more difficult than the electrooxidation of fuels, the large polarization resistance of the cathode is the main obstacle for reducing the operating temperature of SOFCs to the intermediate range.[4] Therefore, the development of new cathode materials with excellent performance (activity and stability) is urgently needed. During the past years, many cobalt-containing perovskite-type oxides, instead of conventional $La_{0.8}Sr_{0.2}MnO_3$ (LSM) compounds, such as $Ba_{0.5}Sr_{0.5}Co_{0.8}Fe_{0.2}O_{3-\delta}$ (BSCF), $La_{0.6}Sr_{0.4}Co_{0.2}Fe_{0.8}O_{3-\delta}$ (LSCF), $PrBaCo_2O_{5+\delta}$ (PBC), $Ba_2Bi_{0.1}Sc_{0.2}Co_{1.7}O_{6-\delta}$ (BBSC), $SrNb_{0.1}Co_{0.7}Fe_{0.2}O_{3-\delta}$ (SNCF), and $SrSc_{0.175}Nb_{0.025}Co_{0.8}O_{3-\delta}$ (SSNC), have been developed, and showed superior catalytic activity in the electrochemical oxygen reduction reaction (ORR) at intermediate temperatures.[5–11] Nevertheless, these materials often suffer from various problems, such as the high thermal expansion coefficients (TECs) that are due to the chemical expansion of the cobalt cations, poor structural stability, inadequate compatibility with the electrolyte, and questionable CO_2 poisoning effects, which limit their practical applications.[12–14] CO_2 tolerance is of particular importance for a cathode working under ambient atmosphere because CO_2 poisoning can significantly deteriorate the performance and long-term durability of cathodes.[14,15] For example, the performance of a symmetric cell with the well-known BSCF cathode decreased by approximately 20 times after the introduction of 10 vol% CO_2 into the air atmosphere at 600 °C for only 5 min.[16] The sensitivity of the above materials to CO_2 poisoning is due to the adsorption of CO_2 or the formation of carbonate species on the surface of perovskites that contain alkaline-earth metals, which can destroy the original phase structure and significantly degrade the surface oxygen exchange kinetics.[14,17,18] Accordingly, a cathode material with good CO_2 tolerance will be of practical value, particularly when applied in portable single-chamber SOFCs. Although some strategies (e.g., decreasing the basicity of the oxide or forming a hierarchical structure) for the development of CO_2-resistant materials have been proposed,[16,19,20] there are still no alkaline-earth-containing cathode materials with complete CO_2 tolerance for intermediate temperature (IT) SOFCs.

Aurivillius phases are layered bismuth-containing oxides with the general formula $Bi_2A_{n-1}B_nO_{3n+3}$, which can alternatively be expressed as $Bi_2O_2[A_{n-1}B_nO_{3n+1}]$ ($n = 1$–5), consisting of n perovskite layers $[A_{n-1}B_nO_{3n+1}]^{2-}$ sandwiched between bismuth–oxygen sheets $[Bi_2O_2]^{2+}$.[21] The Aurivillius oxide family has been the subject of extensive studies aiming towards various applications, such as low-fatigue ferroelectrics, fast oxygen-ion conductors, and photocatalysis.[22–24]

However, very little is known about the use of Aurivillius-type materials as cathodes for IT-SOFCs.

Herein, we report the use of the new cobalt-free $n=3$ Aurivillius oxide $Bi_2Sr_2Nb_2MnO_{12-\delta}$ (BSNM) as an outstanding cathode for IT-SOFCs. The Aurivillius BSNM cathode showed favorable ORR activity at intermediate temperatures in a symmetric cell with $Sm_{0.2}Ce_{0.8}O_{1.9}$ (SDC) as the electrolyte, achieving a relatively low area-specific resistance (ASR) of 0.26 $\Omega\,cm^{-2}$ at 750 °C. An anode-supported single cell with the single-phase BSNM cathode also demonstrated a high peak power density of approximately 1000 $mW\,cm^{-2}$ at 750 °C and operated stably within a test period of 100 h. The ORR activity could be significantly enhanced by forming a BSNM/SDC/Ag composite cathode, which showed an ASR value of only 0.11 $\Omega\,cm^{-2}$ and a higher peak power density of about 1294 $mW\,cm^{-2}$ at 750 °C. Furthermore, the BSNM exhibited a low TEC value of $12.8\times10^{-6}\,K^{-1}$, excellent structural stability, and good chemical compatibility with the electrolyte. More importantly, the BSNM oxide benefits from complete CO_2 tolerance and is the sole alkaline-earth-containing cathode material with this property thus far. These features render the new material a highly promising IT-SOFC cathode for practical applications.

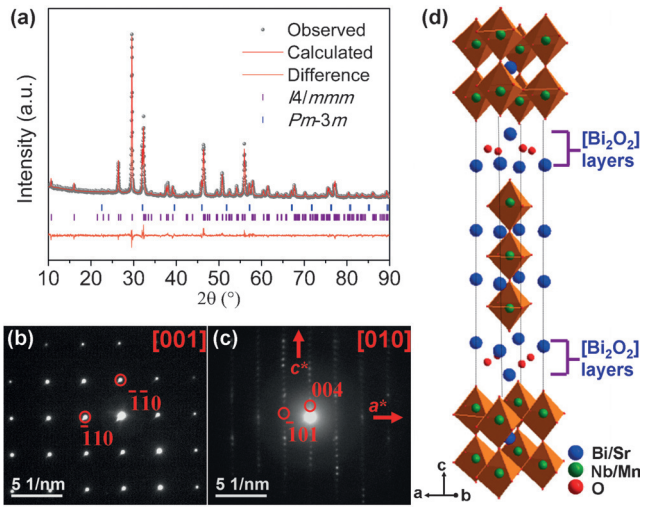

Figure 1. a) Refined XRD profiles of the BSNM sample. b, c) SAED patterns along the [001] and [010] zone axes for the major phase of BSNM. d) Schematic representation of the Aurivillius BSNM crystal structure.

The phase structure of BSNM was first analyzed by room-temperature X-ray diffraction (RT-XRD; Figure 1a). Rietveld refinement revealed that the BSNM consists of a major Aurivillius phase as well as a small amount of a minor perovskite phase, which is consistent with the results reported by Greaves and McCabe.[25] The major Aurivillius phase of BSNM has a tetragonal structure (space group: *I*4/*mmm*) with lattice parameters of $a=b=3.913$ Å and $c=33.08$ Å. The minor perovskite phase $Sr(Mn,Nb)O_3$ has a cubic structure with the space group *Pm*-3*m* (see the Supporting Information, Table S1). The reliability of the Rietveld refinement was confirmed by $R_p=5.68\,\%$, $R_{wp}=7.40\,\%$, and $\chi^2=1.875$, indicating the goodness of fit. The major tetragonal phase structure of BSNM was further confirmed by two key selected-area electron diffraction (SAED) patterns recorded along the [001] and [010] zone axes (Figure 1b,c), and the SAED pattern along the [111] zone axis was indicative of the minor cubic structure (Figure S1). Figure 1d schematically depicts the typical layered Aurivillius phase structure of BSNM.

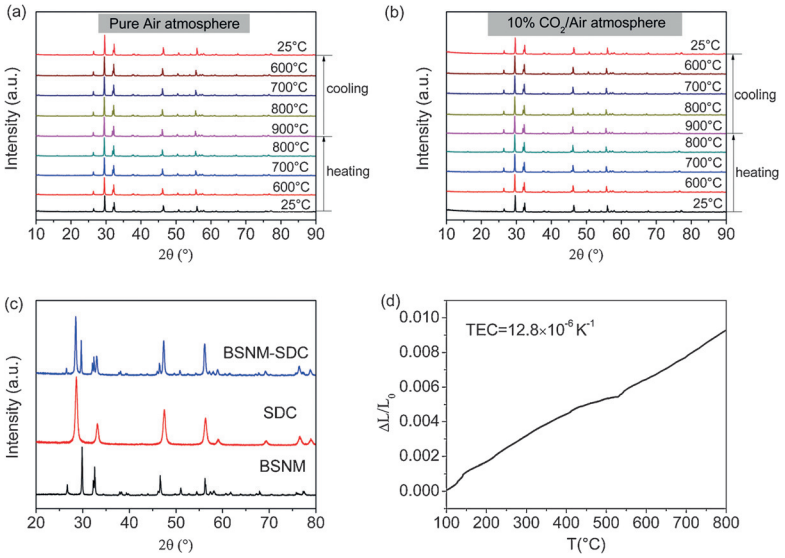

Figure 2. a) High-temperature X-ray diffraction (HT-XRD) patterns of the BSNM powder at 25–900 °C in pure air. b) HT-XRD patterns of the BSNM powder at 25–900 °C in air containing 10 vol% CO_2. c) XRD patterns of a mixture of BSNM and SDC (1:1, w/w) powders calcined at 1000 °C for 2 h. d) Thermal expansion curve of the BSNM sample between 100 and 900 °C in air.

Good structural stability is of great importance to cathode materials during operation. The phase stability of BSNM at elevated temperatures in air was examined by performing in situ X-ray diffraction at temperatures of 25–900 °C upon heating and cooling (Figure 2a). Within this temperature range, the phase structure of BSNM did not change, and phase transformations, or the formation of new phase(s), were not observed. Even in air containing 10 vol% CO_2 (i.e., 10% CO_2/air), the phase structure of BSNM was still stable during heating and cooling (Figure 2b). To evaluate the chemical compatibility of the BSNM cathode with the SDC electrolyte, the phase reaction of the BSNM cathode with the SDC electrolyte was investigated by calcining a mixture of BSNM and SDC powders (1:1, w/w) at 1000 °C for two hours. Based on the XRD patterns shown in Figure 2c, the BSNM and SDC retained their own phase structures as no extra diffraction peaks were detected, indicating that no significant chemical reaction had occurred between the two materials. Figure 2d shows the thermal expansion curve of BSNM between 100 and 800 °C in air. The low TEC value of BSNM ($12.8\times10^{-6}\,K^{-1}$) is much closer to that of the SDC electrolyte ($12.3\times10^{-6}\,K^{-1}$),[26] reducing the risk of the delamination of

the cathode material from the electrolyte during the heating/cooling processes. These advantages of the BSNM cathode are extremely beneficial to the stable operation of SOFCs in practical applications.

The ORR activity of the BSNM cathode was evaluated by electrochemical impedance spectroscopy (EIS) using a symmetric cell with the configuration of BSNM | $Sm_{0.2}Ce_{0.8}O_{1.9}$ (SDC) | BSNM. The area-specific resistance (ASR) value, represented by the difference between the real axes intercepts at the high and low frequencies of each impedance loop, is generally used to reflect the ORR activity of cathodes. Arrhenius plots of the ASRs for BSNM cathodes fired at different temperatures (800–1000 °C) are shown in Figure 3 a. The BSNM cathode fired at 800 °C exhibited the lowest ASR value for all tested temperatures. The firing temperature of the BSNM cathode can be reduced to 800 °C, and increasing the firing temperature leads to a decrease in ORR activity.

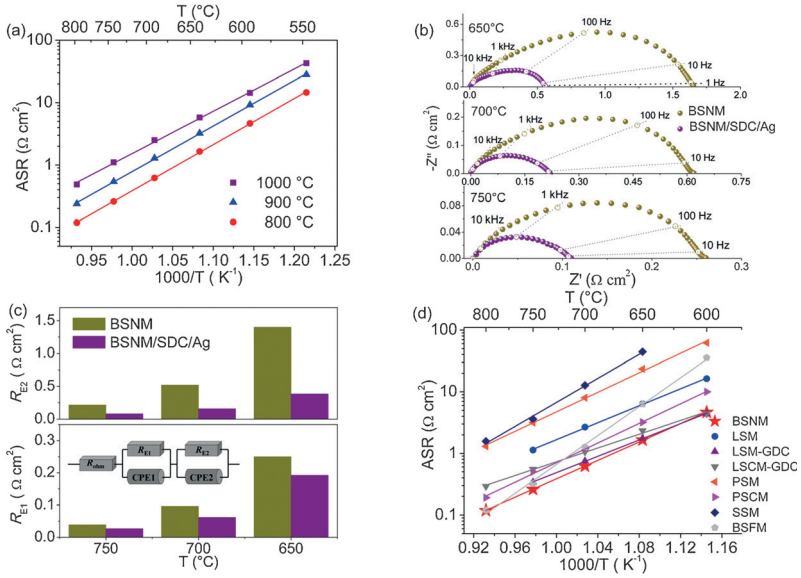

Figure 3. a) Arrhenius plots of the ASRs for BSNM cathodes fired at different temperatures (800, 900, and 1000 °C). b) Nyquist plots of the impedance spectra of BSNM and BSNM/SDC/Ag cathodes fired at 800 °C for 2 h in air at 750, 700, and 650 °C. The ohmic resistance from the electrolyte was subtracted for direct comparison. c) Comparison of the R_{E1} and R_{E2} values for BSNM and BSNM/SDC/Ag cathodes fired at 800 °C for 2 h in the temperature range of 650–750 °C. Inset: the equivalent circuit model. d) Performance mapping of the ASR values of the BSNM cathode against other reported manganese-containing cathodes, such as $La_{0.8}Sr_{0.2}MnO_3$ (LSM),[38] LSM-GDC,[38] $La_{0.8}Sr_{0.2}Mn_{0.8}Cu_{0.2}O_3$-GDC (LSCM-GDC),[39] $Pr_{0.75}Sr_{0.2}MnO_{3-\delta}$ (PSM),[40] $PrSrCoMnO_{6-\delta}$ (PSCM),[40] $Sm_{0.5}Sr_{0.5}MnO_{3-\delta}$ (SSM),[41] and $Bi_{0.7}Sr_{0.3}Fe_{0.5}Mn_{0.5}O_{3-\delta}$ (BSFM).[42]

The higher activity at lower firing temperatures cannot be explained by an interfacial reaction between BSNM and the SDC electrolyte because no phase reaction was observed in the XRD analysis for the BSNM and SDC mixture calcined at 1000 °C (Figure 2 c). Considering that smaller particles have an increased surface area for catalysis, the reduced sinterability with smaller particle sizes for the BSNM cathode at lower temperature (e.g., 800 °C; Figure S2) contributed to the higher ORR activity.

The electrical conductivity of BSNM was also measured by the four-probe direct current (DC) technique. As shown in Figure S3, the electrical conductivity of BSNM is very low (ca. 0.13–0.28 S cm^{-1} at 600–900 °C), which could be the major factor limiting the ORR activity. To address this issue, the addition of a second phase with high electrical conductivity is an effective way to improve the ORR activity. Silver has widely been recognized as the most popular candidate owing to its good catalytic activity, high electrical conductivity, and relatively low price.[27–31] Furthermore, the electrocatalytic activity of a cathode can generally be improved by forming a composite with ceria-based oxides (e.g., SDC) owing to the extension of triple phase boundary (TPB) sites.[32–34] Based on these considerations, we tried to prepare a BSNM/SDC/Ag composite cathode (13.7 wt % Ag, 21.6 wt % SDC, 64.7 wt % BSNM) from a core–shell precursor in a one-step process as reported before.[35] As seen from the SEM image (Figure S4), a porous composite cathode heated at 800 °C was firmly attached to the SDC electrolyte, indicating good thermal compatibility between the composite cathode and the SDC electrolyte. Figure 3 a shows typical impedance spectra of the BSNM and BSNM/SDC/Ag cathodes fired at 800 °C for 2 h in the temperature range of 650–750 °C. As expected, the BSNM/SDC/Ag composite cathode displayed much better ORR activity than the BSNM cathode. The ASRs of the BSNM cathode are 0.26, 0.62, and 1.65 Ω cm^{-2} at 750, 700, and 650 °C, respectively, whereas the corresponding values for the BSNM/SDC/Ag composite cathode are 0.11, 0.22, and 0.58 Ω cm^{-2}, approximately 58–65 % lower. It should be noted that the ORR performance of the BSNM/SDC/Ag composite may be further enhanced by optimizing the component ratio or changing the preparation method to infiltration, for example; such studies will be part of our future work.

Furthermore, to understand the rate-determining process in the ORR for the BSNM cathode, an equivalent circuit model with the R_Ω-(R_{E1}-CPE_1)-(R_{E2}-CPE_2) configuration was used to fit the impedance spectra. In the model, R_Ω is the ohmic resistance from the electrolyte, electrode, and lead; CPE_1 and CPE_2 are the constant phase elements. High-frequency resistance is associated with the charge-transfer process (R_{E1}), whereas low-frequency resistance is ascribed to oxygen surface processes (R_{E2}), including oxygen adsorption–desorption, oxygen dissociation at the gas–cathode interface, and surface diffusion of intermediate oxygen species.[27,36] The fits for R_{E1} and R_{E2} at 650–750 °C are shown in Figure 3 c. The R_{E2} values are higher than the R_{E1} values for the BSNM cathode at all temperatures, suggesting that the oxygen surface process is the rate-determining step on the BSNM cathode for the ORR. The R_{E2} values of the BSNM/SDC/Ag composite cathode were significantly lower, whereas the R_{E1} values were only slightly affected. This result suggests that the Ag and SDC compo-

nents in the BSNM/SDC/Ag composite cathode accelerate the oxygen surface exchange process for the ORR, which is in accordance with previous results.[27,30,33,37] We also compared the electrochemical performance of BSNM with some single-phase manganese-containing cathodes (Figure 3d) as well as other cathodes reported in the literatures (Table S2). The BSNM achieved the lowest ASR values among all compared materials, despite the low electrical conductivity. Notably, the ORR activity of the BSNM/SDC/Ag composite cathode is comparable to that of the well-known $La_{0.6}Sr_{0.4}Co_{0.2}Fe_{0.8}O_{3-\delta}$ (LSCF) cathode (Figure S5).

Apart from the requirement for high catalytic activity in the ORR, good chemical stability against impurities in the surrounding atmosphere is another critical factor for excellent cathodes. As mentioned above, CO_2-poisoning-induced performance degradation is a serious problem for many highly active alkaline-earth-containing cathodes. To determine the tolerance towards CO_2, the ASR value of the BSNM cathode at 700 °C was monitored after the introduction of air containing a high concentration of CO_2 (10 vol %). As shown in Figure 4a, the ASR of the BSNM cathode hardly changed even after having been subjected to CO_2 for as long as 5 h, suggesting that the BSNM tolerates CO_2 extremely well. In contrast, the well-known LSCF and BSCF cathodes exhibited substantial increases in the ASR values (Figure 4b,c). The ASR values of LSCF and BSCF increased by approximately 61 % and 175 %, respectively, after the introduction of 10 vol % CO_2 for only 15 min, indicating serious CO_2 poisoning. Although the ORR activity of BSNM is inferior to that of LSCF and BSCF, the CO_2 tolerance of the former is significantly higher. Furthermore, the CO_2 tolerance of BSNM and LSCF was systematically compared by various techniques, such as thermogravimetric (TG) analysis, Fourier transform infrared (FTIR) spectroscopy, and CO_2 temperature programmed desorption (CO_2-TPD). Excellent agreement among the results (Figure S6) from TG, FT-IR, and CO_2-TPD demonstrated that the BSNM has a much better tolerance to CO_2 than LSCF. The superior CO_2 tolerance of BSNM can be ascribed to the high acidity of Nb^{5+}, Bi^{3+}, and Mn^{3+}/Mn^{4+} in the BSNM oxide,[19,43] as metal oxides with higher acidity tend to be more resistant towards CO_2.[19] However, the method is qualitative rather than quantitative as the acidity value of the metal oxide is uncertain. Instead, the average metal–oxygen bond energy (ABE) of the metal oxides estimated from thermodynamic calculations can serve as a quantitative value to evaluate the CO_2 tolerance of metal oxides.[20,44,45] More negative ABE values denote better CO_2 tolerance.[44] Figure 4d shows the ABE values of BSNM, LSCF, and BSCF, which were calculated to be −414, −316, and −274 kJ mol^{-1}, respectively, suggesting that BSNM has the best CO_2 resistance. In light of the complete CO_2 tolerance of the BSNM oxides, the BSNM/SDC/Ag composite cathode also exhibited superior resistance to CO_2 (Figure S7). The complete CO_2 tolerance of BSNM-based cathodes highlights their practical value in commercial IT-SOFCs.

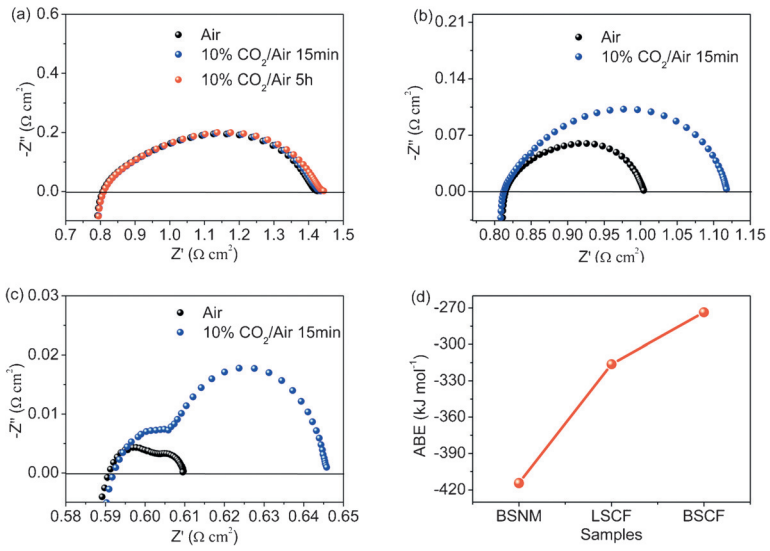

Figure 4. Impedance spectra of a) BSNM, b) LSCF, and c) BSCF cathodes at 700 °C in air and in air containing 10 vol % CO_2. d) The average metal–oxygen bond energies (ABEs) for the BSNM, LSCF, and BSCF cathodes.

Finally, the electrochemical performance of the BSNM cathode fired at 800 °C was further characterized in a nickel/yttrium oxide stabilized zirconium oxide (YSZ-Ni) anode supported YSZ(6 μm) | SDC(2 μm) double-layer electrolyte single cell (for an SEM image, see Figure S8). The voltage and power density polarization curves of the single cell were obtained with hydrogen as the fuel and ambient air as the oxidizing agent between 650 and 800 °C (Figure 5a). The peak power densities of the single cell with the BSNM cathode were 1329, 1001, 647, and 283 mW cm^{-2} at 800, 750, 700, and 650 °C, respectively, indicating the favorable electrochemical performance of the BSNM cathode under real fuel-cell operating conditions. Furthermore, the fuel cell showed a highly stable power output under a constant polarization current density of 1000 mA cm^{-2} at 750 °C for as long as 100 h (Figure 5b). The highly stable electrochemical performance of the BSNM cathode can be ascribed to the low TEC value, the good structural stability and compatibility, and complete CO_2 tolerance as discussed above. The performance of a single cell with the BSNM cathode can be further improved by using the BSNM/SDC/Ag composite cathode. The corresponding single cell gave peak power densities of 1294, 991, and 623 mW cm^{-2} at 750, 700, and 650 °C, respectively, which is comparable to the performance of the well-known LSCF cathode under identical test conditions. A systematic comparison of the single cell performance (peak power density and power density at 0.8 V) of BSNM, BSNM/SDC/Ag, and LSCF is given Table S3.

In summary, the new Aurivillius structure $Bi_2Sr_2Nb_2MnO_{12-\delta}$ (BSNM) was used as a cathode with complete CO_2 tolerance in IT-SOFCs. The BSNM cathode exhibited favorable catalytic activity for the ORR with a low ASR value of 0.26 Ω cm^{-2} at 750 °C. An anode-supported single cell with the BSNM cathode delivered a high peak power density of approximately 1000 mW cm^{-2} at 750 °C and

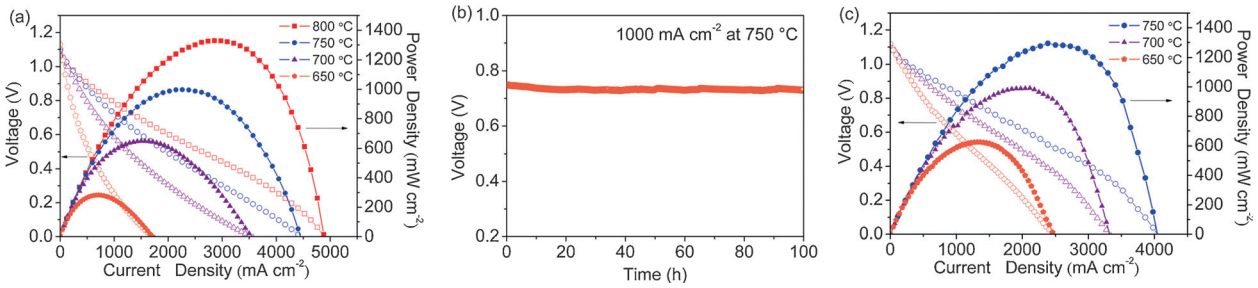

Figure 5. a) *I–V* and *I–P* curves of a single cell based on the BSNM cathode between 650 and 800 °C. b) Time-dependent voltage profile of the single cell operated at a current density of 1000 mA cm^{-2} at 750 °C. c) *I–V* and *I–P* curves of a single cell based on the BSNM/SDC/Ag composite cathode between 650 and 750 °C.

operated stably within a test period of 100 h. The ORR performance could be significantly enhanced by forming a BSNM/SDC/Ag composite cathode as seen by symmetric-cell and single-cell tests. Moreover, the BSNM cathode also has some other advantages, such as a low TEC value, good structural stability, and adequate compatibility with the electrolyte. These results showcase the potential of the new BSNM material as a promising cathode for IT-SOFCs. Aside from the SOFC application, the BSNM material may also be applied in other high-temperature devices, such as oxygen sensors, oxygen pumps, oxygen transport membranes, and reactors.

Acknowledgements

This work was financially supported by the Key Projects in Nature Science Foundation of Jiangsu Province (BK2011030), the National Nature Science Foundation of China (21576135), the Major Project of Educational Commission of Jiangsu Province of China (13KJA430004), the Priority Academic Program Development of Jiangsu Higher Education Institutions, the Changjiang Scholars Program (T2011170), the CAS Interdisciplinary Innovation Team, the Program for Jiangsu Specially-Appointed Professors, and the Youth Fund in Jiangsu Province (BK20150945).

Keywords: Aurivillius oxides · cathodes · electrochemistry · oxygen reduction reaction · solid oxide fuel cells

How to cite: *Angew. Chem. Int. Ed.* **2016**, *55*, 8988–8993
Angew. Chem. **2016**, *128*, 9134–9139

[1] S. Chu, A. Majumdar, *Nature* **2012**, *488*, 294.
[2] B. C. H. Steele, A. Heinzel, *Nature* **2001**, *414*, 345.
[3] E. D. Wachsman, K. T. Lee, *Science* **2011**, *334*, 935.
[4] S. B. Adler, *Chem. Rev.* **2004**, *104*, 4791.
[5] Z. P. Shao, S. M. Haile, *Nature* **2004**, *431*, 170.
[6] E. Perry Murray, M. J. Sever, S. A. Barnett, *Solid State Ionics* **2002**, *148*, 27.
[7] G. Kim, S. Wang, A. J. Jacobson, L. Reimus, P. Brodersen, C. A. Mims, *J. Mater. Chem.* **2007**, *17*, 2500.
[8] W. Zhou, J. Sunarso, Z.-G. Chen, L. Ge, J. Motuzas, J. Zou, G. X. Wang, A. Julbe, Z. H. Zhu, *Energy Environ. Sci.* **2011**, *4*, 872.
[9] Y. L. Zhu, Z.-G. Chen, W. Zhou, S. S. Jiang, J. Zou, Z. P. Shao, *ChemSusChem* **2013**, *6*, 2249.
[10] Y. L. Zhu, J. Sunarso, W. Zhou, S. S. Jiang, Z. P. Shao, *J. Mater. Chem. A* **2014**, *2*, 15454.
[11] W. Zhou, J. Sunarso, M. W. Zhao, F. L. Liang, T. Klande, A. Feldhoff, *Angew. Chem. Int. Ed.* **2013**, *52*, 14036; *Angew. Chem.* **2013**, *125*, 14286.
[12] S. Švarcová, K. Wiika, J. Tolcharda, H. J. M. Bouwmeesterb, T. Grandea, *Solid State Ionics* **2008**, *178*, 1787.
[13] W. Zhou, R. Ran, Z. P. Shao, W. Q. Jin, N. P. Xu, *J. Power Sources* **2008**, *182*, 24.
[14] E. Bucher, A. Egger, G. B. Caraman, W. Sitte, *J. Electrochem. Soc.* **2008**, *155*, B1218.
[15] A. Y. Yan, M. J. Chen, Y. L. Dong, W. S. Yang, V. Maragou, S. Q. Song, P. Tsiakaras, *Appl. Catal. B* **2006**, *66*, 64.
[16] W. Zhou, F. L. Liang, Z. P. Shao, Z. H. Zhu, *Sci. Rep.* **2012**, *2*, 327.
[17] A. Y. Yan, V. Maragou, A. Arico, M. J. Chen, P. Tsiakaras, *Appl. Catal. B* **2007**, *76*, 320.
[18] Z. Zhao, L. Liu, X. M. Zhang, B. F. Tu, D. R. Ou, M. J. Cheng, *Int. J. Hydrogen Energy* **2012**, *37*, 19036.
[19] J. X. Yi, M. Schroeder, T. Weirich, J. Mayer, *Chem. Mater.* **2010**, *22*, 6246.
[20] Y. L. Zhu, J. Sunarso, W. Zhou, Z. P. Shao, *Appl. Catal. B* **2015**, *172*, 52.
[21] B. Aurivillius, *Ark. Kemi* **1949**, *1*, 499.
[22] C. H. Hervoches, A. Snedden, R. Riggs, S. H. Kilcoyne, P. Manuel, P. Lightfoot, *J. Solid State Chem.* **2002**, *164*, 280.
[23] K. R. Kendall, C. Navas, J. K. Thomas, H.-C. zur Loye, *Chem. Mater.* **1996**, *8*, 642.
[24] D. Wang, K. Tang, Z. H. Liang, H. G. Zheng, *J. Solid State Chem.* **2010**, *183*, 361.
[25] E. E. McCabe, C. Greaves, *J. Mater. Chem.* **2005**, *15*, 177.
[26] S. Y. Li, Z. Lü, B. Wei, X. Q. Huang, J. P. Miao, Z. G. Liu, W. H. Su, *J. Alloys Compd.* **2008**, *448*, 116.
[27] W. Zhou, R. Ran, Z. P. Shao, R. Cai, W. Q. Jin, N. P. Xu, J. Ahn, *Electrochim. Acta* **2008**, *53*, 4370.
[28] F. L. Liang, W. Zhou, J. Li, Z. H. Zhu, *J. Mater. Chem. A* **2013**, *1*, 13746.
[29] F. L. Liang, W. Zhou, Z. H. Zhu, *ChemElectroChem* **2014**, *1*, 1627.
[30] Y. L. Zhu, W. Zhou, R. Ran, Y. B. Chen, Z. P. Shao, M. L. Liu, *Nano Lett.* **2016**, *16*, 512.
[31] S. P. Simner, M. D. Anderson, J. E. Coleman, J. W. Stevenson, *J. Power Sources* **2006**, *161*, 115.
[32] J. D. Zhang, Y. Ji, H. B. Gao, T. M. He, J. Liu, *J. Alloys Compd.* **2005**, *395*, 322.
[33] D. J. Chen, R. Ran, Z. P. Shao, *J. Power Sources* **2010**, *195*, 7187.
[34] J. Kim, W. Y. Seo, J. Shin, M. L. Liu, G. Kim, *J. Mater. Chem. A* **2013**, *1*, 515.
[35] Y. J. Niu, F. L. Liang, W. Zhou, J. Sunarso, Z. H. Zhu, Z. P. Shao, *ChemSusChem* **2011**, *4*, 1582.

[36] E. P. Murray, T. Tsai, A. Barnett, *Solid State Ionics* **1998**, *110*, 235.
[37] Y. J. Zhou, Z. Lü, P. Z. Gao, Y. T. Tian, X. Q. Huang, W. H. Su, *J. Power Sources* **2012**, *209*, 158.
[38] E. Perry Murray, S. A. Barnett, *Solid State Ionics* **2001**, *143*, 265.
[39] T. Noh, J. Ryu, R. O'Hayre, H. Lee, *Solid State Ionics* **2014**, *260*, 30.
[40] D. Ding, M. F. Liu, Z. B. Liu, X. X. Li, K. Blinn, X. B. Zhu, M. L. Liu, *Adv. Energy Mater.* **2013**, *3*, 1149.
[41] F. F. Dong, D. J. Chen, R. Ran, H. Park, C. Kwak, Z. P. Shao, *Int. J. Hydrogen Energy* **2012**, *37*, 4377.
[42] D. Baek, A. Kamegawa, H. Takamura, *Solid State Ionics* **2013**, *253*, 211.
[43] N. C. Jeong, J. S. Lee, E. L. Tae, Y. J. Lee, K. B. Yoon, *Angew. Chem. Int. Ed.* **2008**, *47*, 10128; *Angew. Chem.* **2008**, *120*, 10282.
[44] J. X. Yi, J. Brendt, M. Schroeder, M. Martin, *J. Membr. Sci.* **2012**, *387–388*, 17.
[45] Y. Zhang, G. M. Yang, G. Chen, R. Ran, W. Zhou, Z. P. Shao, *ACS Appl. Mater. Interfaces* **2016**, *8*, 3003.

Received: April 28, 2016
Published online: June 13, 2016

